Food Chemistry: X 24 (2024) 101911

Contents lists available at ScienceDirect

Food Chemistry: X

journal homepage: www.sciencedirect.com/journal/food-chemistry-x

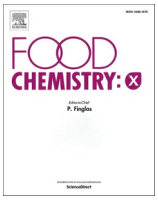

A clenbuterol detection method based on magnetic separation up-conversion fluorescent probe

Xin-Jie Song [a,1], Fei Ye [a,1], Yao Zhang [a], Juan Sun [a], Xuping Shentu [b], Xiaoping Yu [b], Wei Li [c], Yuan-Feng Wu [a,*]

[a] Zhejiang Provincial Key Laboratory of Chemical and Biological Processing Technology for Agricultural Products, School of Biological and Chemical Engineering, Zhejiang University of Science and Technology, Liuxia Street Number 318, Hangzhou 310023, PR China
[b] Zhejiang Provincial Key Laboratory of Biometrology and Inspection and Quarantine, College of Life Science, China Jiliang University, Hangzhou, China
[c] Korean Medicine (KM) Application Center, Korea Institute of Oriental Medicine, Daegu 41062, Republic of Korea

ARTICLE INFO

Keywords:
Clenbuterol
Detection method
Aptamer
Up-conversion nanoparticles
Magnetic nanoparticles

ABSTRACT

In this study, a fluorescence detection method combining aptamer-modified up-conversion nanoparticles (UCNPs) and magnetic nanoparticles (MNPs) was developed for detection of Clenbuterol (CLB). The aptamer-modified magnetic NPs captured CLB, which reacted with the aptamer-modified UCNPs and generated a sandwich complex. The aptamer-modified UCNPs acted as a fluorescence source. The MNP-CLB-UCNP complex was retrieved from the solution using an magnetic field, and the fluorescence intensity was detected by fluorescence spectrophotometry with excitation and emission spectra at 980 nm and in the 400–800 nm region, respectively. The results showed that the fluorescence intensity gradually increased with increasing concentrations of CLB with a good specify. The method was highly sensitive for the quantification of CLB, with a limit of detection of 0.304 ng mL^{-1}. The recovery rate of CLB from pork samples ranged from 84 % to 94.87 %. This fluorescence method enables the sensitive, precise, and accurate quantification of CLB residues in pork samples.

1. Introduction

Clenbuterol (CLB) is a β-receptor agonist used clinically to treat bronchial spasms caused by respiratory diseases, such as bronchial asthma, asthmatic bronchitis, and emphysema. In the early 1980s, Cyanamid, an American chemical company, accidentally found that clenbuterol clearly promoted growth, increased the lean meat rate, and reduced fat; therefore, it was used in animal husbandry (Rubio et al., 2020). CLB acts on β2 adrenergic receptors and increases adenosine cyclophosphate levels by activating adenylate cyclase, thereby enhancing lipolysis, promoting protein synthesis, and stimulating muscle growth, hence greatly increasing the percentage of lean meat (Py et al., 2015). Therefore, CLB was widely used in animal husbandry. The dose of CLB applied was strictly controlled to avoid any significant harm to humans. In contrast, when used illegally, the dose is 5–10 times of that used as a drug; hence large amounts of clenbuterol remains in meat products, especially in the organs. CLB begins to decompose upon heating at 172 °C; hence conventional cooking methods cannot eliminate residual CLB. Post consumption of meat products containing CLB residues, the compound immediately circulates through the human body, causing acute or chronic poisoning, including flushed complexion, headache, dizziness, fatigue, chest tightness, palpitations, skeletal muscle tremors, and limb numbness. In 1997, the Chinese government banned the use of β-adrenergic hormones, including CLB hydrochloride, in feed and animal husbandry production by the Notice on the Prohibition of Illegal Use of Veterinary Drugs (Zhang, Wang, & Su, 2016).

CLB continues to be sold illegally and used in animal husbandry, even though it violates relevant laws and regulations. This is driven by the huge profits that can be achieved with its use (Midkiff, 2004). Long-term CLB consumption may cause chromosomal aberrations that can induce the development of malignant tumors. Because CLB pose a serious threat to human health, its detection and supervision have become important issues in food safety (Liu et al., 2017). Rapid and accurate detection of CLB is particularly important. The available detection methods of CLB include mass spectrometry (MS) (Xiao et al., 2016), liquid chromatography–tandem mass spectrometry (LC-MS/MS) (Zhang, Lu, Zhang, & Wang, 2023), high performance liquid chromatography (HPLC) (Li et al., 2018), gas chromatography tandem mass

* Corresponding author.
E-mail address: wuyuanfeng@zju.edu.cn (Y.-F. Wu).
[1] First Author.

https://doi.org/10.1016/j.fochx.2024.101911
Received 27 June 2024; Received in revised form 14 October 2024; Accepted 19 October 2024
Available online 21 October 2024

spectrometry (GC–MS/MS) (Song et al., 2019), liquid chromatography-mass spectrometry (LC-MS) (Yikilmaz et al., 2020), supercritical fluid chromatography (SFC) (Herpin, Bichon, Rambaud, Monteau, & Le Bizec, 2018), capillary electrophoresis (Wang et al., 2015), enzyme-linked immunosorbent assay (Li et al., 2023; Ma, Nilghaz, Choi, Liu, & Lu, 2018), surface enhanced Raman spectroscopy (Su et al., 2021; Guo et al., 2023;), molecular imprinting (Jin et al., 2018), and electrochemical sensor methods (Jing, Ouyang, Li, & &Long, 2022; Ma, Li, Li, Feng, & Ye, 2022).

Fluorescent detection methods offer advantages such as high analytical sensitivity, strong selectivity, and simplicity (Sargazi et al., 2022). Upconversion nanoparticles (UCNPs) are novel fluorescent materials that can be used to develop new detection methods (Himmelstoß & Hirsch, 2019; Zhao, 2019). UCNPs have broad biomedical application prospects owing to their significant advantages, including light-stability, high chemical stability, low potential toxicity, deep light penetration, depth of penetration, absence of background light interference, and almost no damage to biological tissues (Bastos et al., 2022; Du, Feng, Gao, & Zhang, 2022; Liu et al., 2018; Rafique, Kailasa, & Park, 2019). UCNPs have also been used for fluorescence detection (Jin et al., 2023; Zeng et al., 2024; Zhao et al., 2024). Fluorescence analysis can be combined with immunoassays. However, the cost of antibody preparation is high; besides, antibodies have complex structures and large molecular volumes (Mason et al., 2021). In recent years, with the development of screening technologies, an increasing number of molecules with high affinities and specificities have been identified. An aptamer involves the systematic evolution of ligands using exponential enrichment (SELEX) in vitro screening. The obtained structured oligonucleotide sequence (RNA or DNA) has strict recognition properties and high affinity for the corresponding target molecules (proteins, viruses, bacteria, cells, heavy metal ions, etc.) (Bayat et al., 2018; Zon, 2022). Aptamers have a stronger specificity than antibodies. They have a comparable or even higher affinity for the target molecule than an antibody. Their synthesis and preparation are simple and inexpensive and their stability is better than that of antibodies, making them convenient for storage.

In this study, the CLB aptamer was modified on the surface of amino-modified UCNPs and amino-modified ferro-ferric oxide. The diluted CLB was then combined with the clenbuterol aptamer- and amino-modified ferro-ferric oxide. This was then combined with the aptamer-modified UCNPs. Finally, the preparation was dispersed in phosphate-buffered saline (PBS), and the fluorescence intensity was measured using excitation and emission wavelengths of 548 and 980 nm, respectively, to detect the CLB concentration (Fig. 1). (See Tables 1 and 2.)

2. Materials

2.1. Reagents and instruments

Ferric chloride hexahydrate, 1,6-hexamethylenediamine was purchased from Shanghai McLean Biochemical Technology Co., Ltd.; ethylene glycol, absolute ethanol, methanol, sodium hydroxide were ordered from Shanghai Ling-feng Chemical Reagents Co., Ltd., yttrium chloride, ytterbium chloride, erbium chloride, 1-octadecene (ODE), ammonium fluoride, isopropanol, clenbuterol, estradiol, enrofloxacin were ordered from Aladdin Reagents Co., Ltd., sodium acetate was ordered from Shantou Xi-long Chemical Plant Co., Ltd., 0.01 mol L^{-1} pH 7.4 phosphate buffer (PBS), oleic acid (OA), 3-aminopropyltriethoxysilane (APTES), tetraethyl orthosilicate, tetracycline, salbutamol, Potassium Sorbate, tetraethyl orthosilicate, CLB aptamer was ordered from Shanghai Bioengineering Co., Ltd. The aptamer sequence was 5′-NH2-AGCAGCACAGGTCAGATGTCATCTGAAGTGAATGAAGGTAAA-CATTATTTCATTAACCTATGCGTGCTACCGTGAA-3′. The morphology of the particles was determined by transmission electron microscope (TEM)using a JEM-2100F microscope (JEOL Ltd.) and by scanning electron microscope (SEM) using an SU1510 microscope (Hitachi Ltd.). X-ray diffraction (XRD) was performed using an Ultima IV X-ray diffractometer (Rigaku). Infrared spectra were recorded by BRKER Fourier- transform infrared spectrometry (FTIR) using a Bruker apparatus. The fluorescence signals were measured using an F-4500 fluorescence spectrophotometer (from Hitachi)., Japan. The laser emitter

Table 1
Determination of CLB in pork samples with developed method.

Added (ng mL^{-1})	Amount found (ng mL^{-1})	R.S·D(%)	Recovery(%)
0.1	0.08936	0.2426	89.36
1	0.9487	0.3623	94.87
10	9.001	0.9819	90.01
100	87.84	0.242	87.84
1000	840.02	1.139	84
10,000	8799.03	0.6159	87.99

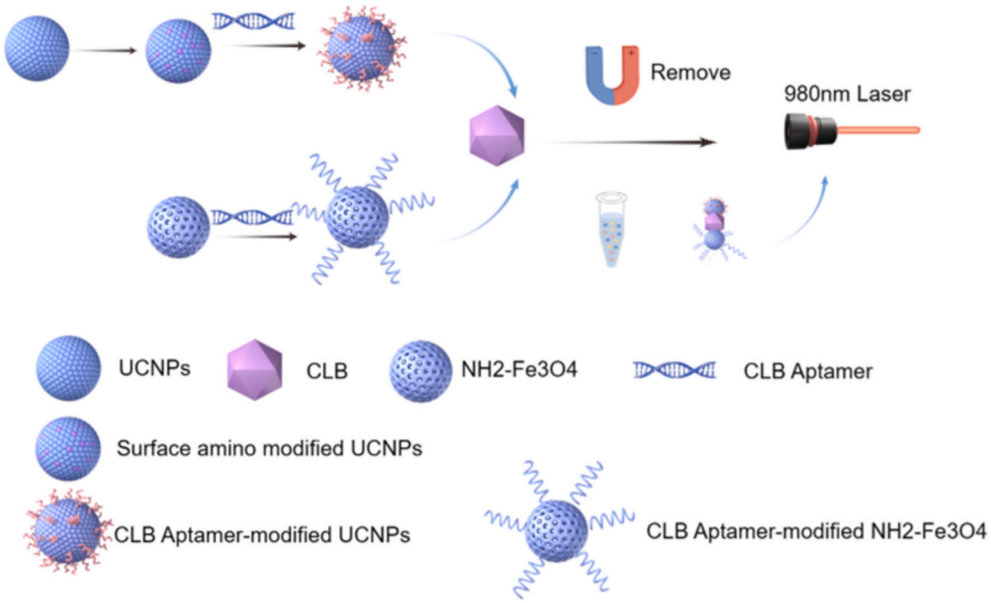

Fig. 1. Schematic of illustration the principle of detection of clenbuterol.

Table 2
Determination of CLB in pork samples with GC–MS.

	Added(ng·mL^{-1})	Measured	%RSD	Recovry(%)
Low	200	184	6.124	92
Medium	400	402.4	8.65	100.6
High	800	812.4	4.206	101.55

used was a 980 nm laser from Beijing Hong-Lan Optoelectronics Technology Co., Ltd.

2.2. Preparation of amino ferro-ferric oxide

The preparation method was based on an established one-step synthesis (Dou, Xiang, Liang, & Liu, 2021). A mixture of 2.0 g sodium acetate, 1.0 g ferric chloride hexahydrate, and 6.5 g 1,6-ethylenediamine dissolved in 30 mL ethylene glycol was heated, stirred, transferred to a 100 mL reactor, and placed in a vacuum drying oven at 190 °C for 10 h. After the reaction was complete, the reaction kettle was cooled and the supernatant was removed by magnetic separation with an external magnetic field to retain the black solid. The black product was washed several times with deionized water and absolute ethanol, and then dried in a vacuum drying oven at 60 °C overnight to obtain aminated ferric oxide.

2.3. Preparation of UCNPs

UCNPs were synthesized as previously described, with slight modifications (Amouroux, Roux, Micheau, Gauffre, & Coudret, 2019). A mixture of 0.78 mmol yttrium chloride, 0.2 mmol ytterbium chloride, and 0.02 mmol erbium chloride, along with oleic acid and 1-octadecene, were added to a 100-mL three-necked flask. The mixture was stirred at 160 °C for 30 min and subsequently allowed to cool. Then, a 10-mL methanol solution containing 2.5 mmol NaOH and 3.9 mmol NH_4F was added. After stirring for 30 min, the mixture was heated to 100 °C for 1 h under an argon atmosphere. The sample was then heated to 300 °C for 1 h under argon protection, and finally cooled to room temperature. The product was collected, precipitated using anhydrous ethanol, and centrifuged at 10,000 rpm for 10 min. The precipitated product was collected, washed several times with cyclohexane, and dried at 60 °C in a vacuum drying oven.

2.4. Surface amino modification of UCNPs

Owing to the hydrophobicity of unmodified UCNPs, their surface modification is usually performed to improve surface activity and realize biological applications. First, 20 mg of UCNPs were added to 60 mL of isopropanol and ultrasonicated for 30 min (Liu et al., 2023). Subsequently, 20 mL distilled water and 2.5 mL 25 % ammonia were added, and the mixture was stirred for 15 min. Then, 20 mL isopropanol and 60 μL tetraethyl orthosilicate were added, and the reaction was performed for 3 h. Following this, 30 mL isopropanol and 200 μL APTES were added, and the reaction was performed for 1 h. The mixture was then incubated at room temperature for 2 h. After centrifugation, the supernatant was discarded and the final product was obtained. The product was washed several times with deionized water and dried in a vacuum oven at 60 °C to obtain amino-modified UCNPs.

2.5. Surface aptamer modification of amino ferro-ferric oxide

Amino-Fe_3O_4 (2 mg) was ultrasonically treated in 1 mL PBS (0.01 mol L^{-1} pH 7.4) for 30 min, followed by the addition of 250 μL 25 % glutaraldehyde solution. The preparation was shaken at 25 °C at 100 rpm for 2 h. The amino-Fe_3O_4 was separated using a magnetic force, washed with PBS, and dispersed in 1 mL of PBS. After ultrasonic treatment for 5 min, 20 μL of 25 μM CLB aptamer solution was added and reacted overnight at 37 °C at 100 rpm. After the reaction, functionalized magnetic NPs were obtained by magnetic separation. After washing with PBS multiple times, the NPs were dispersed in 1 mL PBS (0.01 mol L^{-1} pH 7.4) and stored in a refrigerator at 4 °C.

2.6. Surface aptamer modification of UCNPs

After surface-modified UCNPs (6 mg) were ultrasonically treated in 1 mL PBS (0.01 mol L^{-1} pH 7.4) for 30 min, 250 μL of 25 % glutaraldehyde solution was added to it, and the reactant was oscillated at room temperature for 2 h. Then, the reactant was separated by centrifugation at 12,000 rpm for 10 min. The separation was washed with PBS and dispersed in 1 mL of PBS by a 10-min ultrasonic treatment. After that, 40 μL of 25 μM CLB aptamer solution was added to the UNCPs dispersion and reacted overnight at 37 °C under oscillating condition. At the end of the reaction, the aptamer-modified UCNPs were separated by centrifugation at 12,000 rpm for 10 min. The aptamer-modified UCNPs were washed and dispersed in 1 mL PBS (0.01 mol L^{-1} pH 7.4), and stored in a refrigerator at 4 °C.

2.7. Sample pre-treatment and detection procedure of clenbuterol

Standard CLB solutions of 1, 10, 100, and 1000 ng mL^{-1} were used. Methanol was used as the blank control as the CLB was dispersed in it. The CLB solution was mixed with 100 μL of aptamer-modified Fe_3O_4 and reacted at 37 °C and 100 rpm for 1 h under shaking. After the reaction, CLB-apt-Fe_3O_4 was separated by magnetic separation and washed three times with PBS. Then, 100 μL of aptamer-modified UCNPs were added and reacted at 37 °C for 1 h under shaking, next, the mixture was centrifuged at 12,000 rpm for 10 min, washed three times with PBS, and finally dispersed in 1 mL PBS. The fluorescent intensity was measured using the excitation and emission wavelengths of 980 and 548 nm, respectively.

2.8. Real pork sample analysis

The developed method was also confirmed using spiked real pork samples, and sample pretreatment was performed as previously described (Duan et al., 2020). The spiked samples were analyzed using the developed method and the National Standard of China GBT 5009.192-2003.

2.9. Statistical analysis

The detection limit was calculated according to the International Union of Pure and Applied Chemistry (IUPAC) method (Allegrini, Olivieri, & C., 2014; Amouroux et al., 2019), All experiments and results were analyzed in at least three trials to achieve reliable and reproducible data.

3. Results and discussion

3.1. Detection principle

The aptamer had a high degree of specific recognition; CLB aptamer-modified Fe_3O_4 was used as the capture probe, and CLB aptamer-modified UCNPs were used as the signal probe. In the presence of CLB, CLB aptamer-modified Fe_3O_4, CLB, and CLB aptamer-modified UCNPs formed a sandwich complex with Fe_3O_4_apt-UNCPs. The sandwich complex was separated using a magnetic field. The fluorescence signal was measured using the excitation and emission wavelengths of 980 and 548 nm, respectively.

3.2. Characterization of NH_2-Fe_3O_4

The synthesized NH_2-Fe_3O_4 was characterized by SEM, XRD, and

FTIR. As shown in Fig. 2a, the characteristic absorption peak of Fe—O at 582 cm^{-1}, stretching vibration of the C—H bond at 1036 cm^{-1}, bending of the N—H bond at 1640 cm^{-1}. A wide peak at 3430 cm^{-1} were evident, which may have been caused by the water content due to insufficient drying during the preparation of potassium bromide tablets. The XRD results presented in Fig. 2b were consistent with the XRD standard card for NH_2-Fe_3O_4. SEM revealed that the prepared samples were spherical (Fig. 2c). These collective findings indicated the successful synthesis of NH_2-Fe_3O_4.

3.3. Characterization of UCNPs and NH_2-UCNPs

The UCNPs and surface-amino-modified UCNPs were characterized by SEM, TEM, XRD and FTIR. TEM revealed a nearly hexagonal structure. The XRD results showed that the position of the diffraction peak of the product was consistent with that of the $NaYF_4$ standard. The FTIR results showed nitrogen hydrogen stretching vibration at a wavenumber of approximately 3414 cm^{-1}. At 2927 cm^{-1}, stretching of the carbon-hydrogen bonds occurred at 2927 cm-1. At approximately 1630 cm^{-1}, the bending of nitrogen hydrogen bonds was evident. At 1466 cm^{-1}, bending of carbon hydrogen bonds was indicated. The TEM images of the surface-modified UCNPs revealed a coating layer around the NPs (Fig. 2e). The FT-IR spectra are shown in Fig. 2f. The surface-modified UCNPs exhibited a stretching vibration of the Si—O bond at 1092 cm^{-1} and a bending vibration peak of the nitrogen hydrogen bond at 1630 cm^{-1}, indicating that the UCNPs were successfully modified.

3.4. Aptamer modification of NH_2-Fe_3O_4 and UCNPs

The aptamer exhibited a strong characteristic absorption peak at 260 nm, resulting in absorption peaks at 260 nm for both the aptamer-modified apt-UCNPs and aptamer-modified Fe_3O_4. As shown in Fig. 3, the nanomaterials without an aptamer had no characteristic absorption peak at 260 nm, whereas the modified nanomaterials showed strong absorption at 260 nm, which indicated that the aptamer was successfully coupled to the surface of UCNPs and Fe_3O_4.

3.5. Optimization of the method

The synthesis procedure for UCNPs was optimized (Supplementary Material Fig. S1 and S2). The optimization of the detection method is presented in the Supplementary Material (Fig. S3, S4).

3.6. Analytical performance

According to this detection principle, the CLB aptamer-modified amino ferric oxide specifically recognized and captured CLB. In the presence of CLB aptamer-modified UCNPs, a sandwich complex was formed between the CLB aptamer-modified amino ferric oxide and CLB. The complex was removed by magnetic separation, and the fluorescence signal intensity was detected. As shown in Fig. 4a, the fluorescence signal of the blank control group was the weakest and the fluorescence signal intensity gradually increased with increasing CLB concentration. As shown in Fig. 4b, linear fitting analysis of the data revealed that the linear regression coefficient between the fluorescence intensity and concentration was 0.9924, and the linear regression equation was $y = 285.49x + 262.58$ at the concentrations ranging from 0 to 10,000 ng mL^{-1} (here the data are the fluorescence signal intensities at any concentration minus the fluorescence signal intensity of the blank sample). These findings indicate that this method can detect CLB. As shown in Fig. 4c, the fluorescence intensity gradually increased with an increasing concentration of CLB added to the pork loin. The recovery rate of CLB in

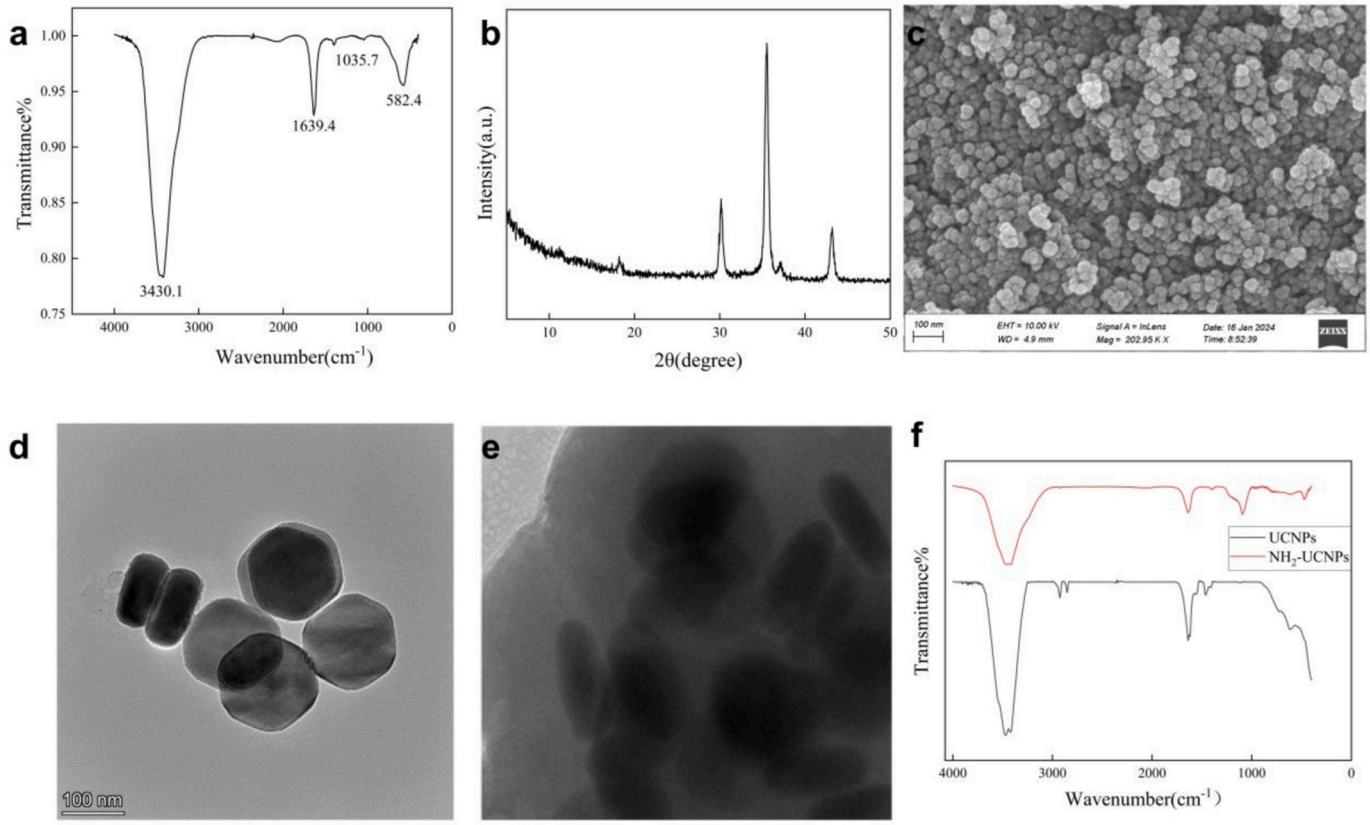

Fig. 2. (a) FTIR spectra of amino-Fe_3O_4; (b) XRD spectra of amino-Fe_3O_4; (c) SEM images of amino ferro-ferric oxide; (d) SEM images of up-conversion nanoparticles; (e) TEM images of surface modified up-conversion nanoparticles; (f) Infrared spectra of up-conversion nanoparticles and surface modified up-conversion nanoparticles.

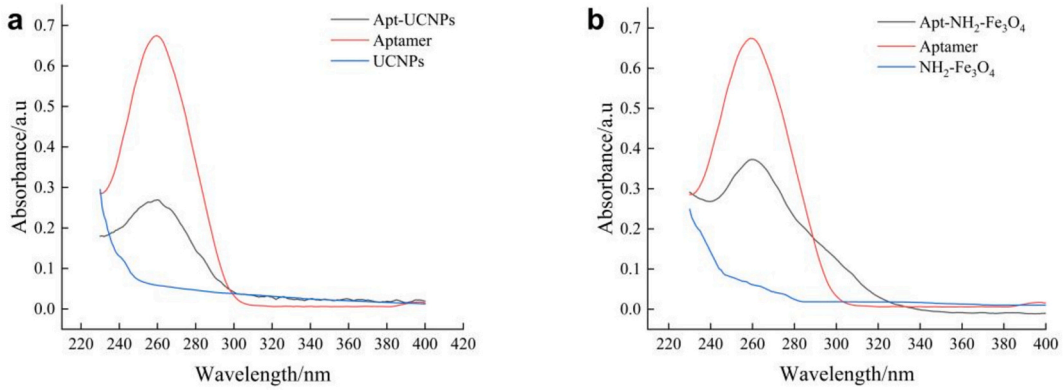

Fig. 3. The UV absorption spectra of (a)Aptamer, Apt-UCNPs and amino-UCNPs (b)Aptamer, Apt-NH_2-Fe_3O_4 and NH_2-Fe_3O_4.

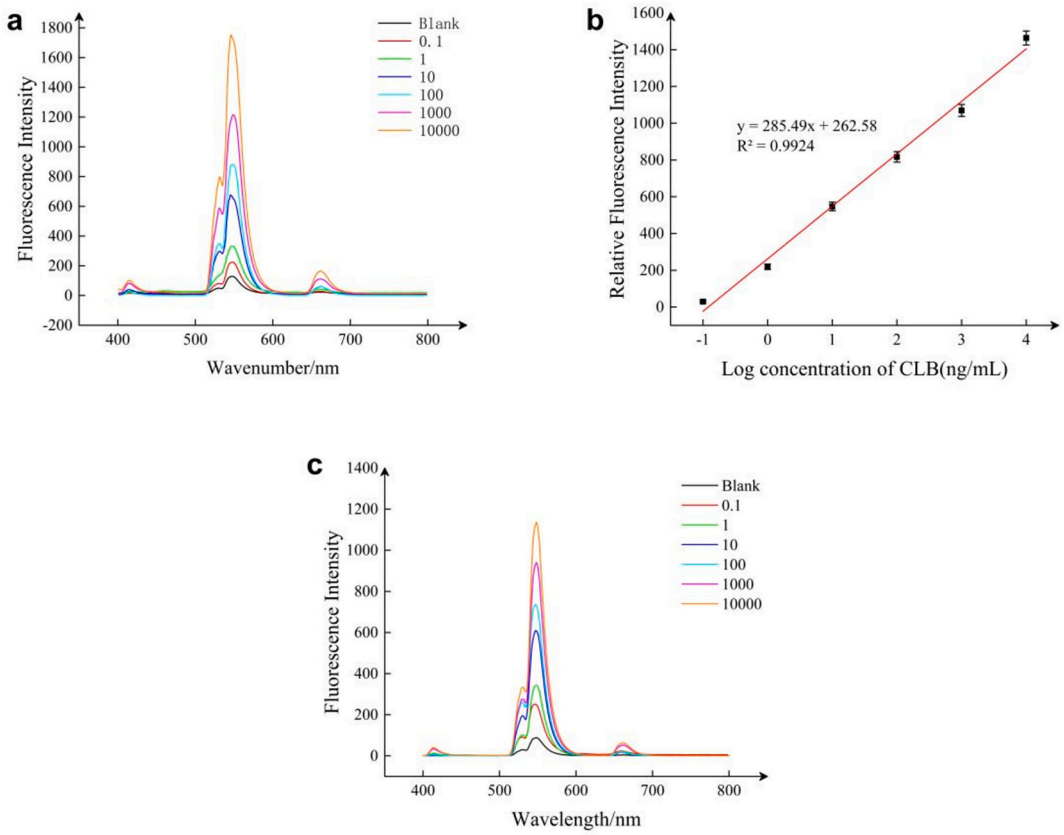

Fig. 4. (a)Fluorescence detection results of clenbuterol at different concentrations; (b) Linear relationship between clenbuterol concentration and fluorescence intensity; (c) The fluorescence intensity of each concentration of CLB was added to the actual pork sample.

the samples was 84 % to 94.87 % (Table 1), indicating that this method is also applicable for actual sample detection. From Table S1, it is evident that when compared to other reported detection methods, the developed fluorescent probe detection method exhibits a lower detection limit and does not require complex derivatization processes, making it simpler to operate.

3.7. Specificity verification

To test the specificity of this method, enrofloxacin, estradiol, tetracycline, salbutamol, and potassium sorbate were selected for further studies. Both NPs were diluted with a concentration gradient of CLB to l, 10, 100, and 1000 ng ml^{-1}. A blank control containing methanol was used. To eliminate unstable factors, CLB, enrofloxacin, estradiol, tetracycline, salbutamol, and potassium sorbate were added together, and fluorescence detection was then performed. In each group, at the same concentration, the fluorescence intensity of CLB was the highest, and the blank control had a weak fluorescence signal. The fluorescence signals of the five groups treated with enrofloxacin, estradiol tetracycline, salbutamol, and potassium sorbate were found to be only slightly higher than that of the blank control group. The fluorescence intensities of these five groups did not change significantly with increasing concentrations, with only a weak fluorescence signal being evident, whereas the fluorescence intensity of CLB changed significantly with increasing concentration. (Fig. 5c). Therefore, it can be concluded that the detection method is specific for CLB and that specific recognition does not occur for other substances.

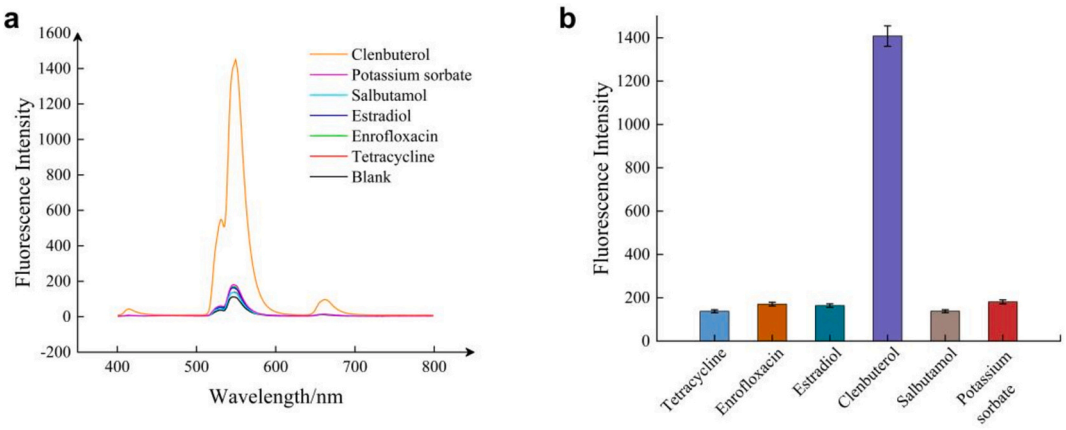

Fig. 5. (a) Fluorescence intensity test results of blank, estradiol, enrofloxacin, tetracycline, salbutamol, potassium sorbate and CLB at different concentrations; (b) Specificity of the detection methods.

3.8. Comparison of the developed method and classical method

The spiked samples with CLB concentration of 200, 400, 800 ng mL^{-1} were analyzed by GC–MS method according to the National Standard of China, Determination of Clenbuterol Residues in Animal-Derived Foods - National Standard of the People's Republic of China GB/T 5009.192-2003. The characteristic peaks of CLB were screened from the mass spectra at *m/z* 86, 187, 243, and 262, as shown in Fig.S5 and S7. Characteristic peaks of metoprolol were observed at m/z 72 and 223, as shown in Fig. S6 and S8. The standard curve of the peak area ratio versus concentration ratio was y = 7.5553x + 0.2062 with R^2 = 0.9929 (Fig. 6). The limit of detection (LOD) and quantification (LOQ) were 0.105 and 0.35 ng mL^{-1}. (LOD = 3 Noise/RF, LOQ = 10 Noise/RF, where Noise is the peak area of the background noise and RF is the response factor of the internal standard). The recovery rates of CLB in the pork samples were studied with concentrations of 200, 400, and 800 ng mL^{-1}. As shown in Table 2, the recovery rates ranged from 92 to 101.55 %. When compared with the developed fluorescence method, the GC–MS method had a better recovery rate, but it was more complex, especially the derivatization process, which was not only cumbersome but also required high operational skills and involved various hazardous chemicals. Compared with the GC–MS method, the developed fluorescence method is simple and easy to handle, not only in the sample preparation steps but also in the analysis.

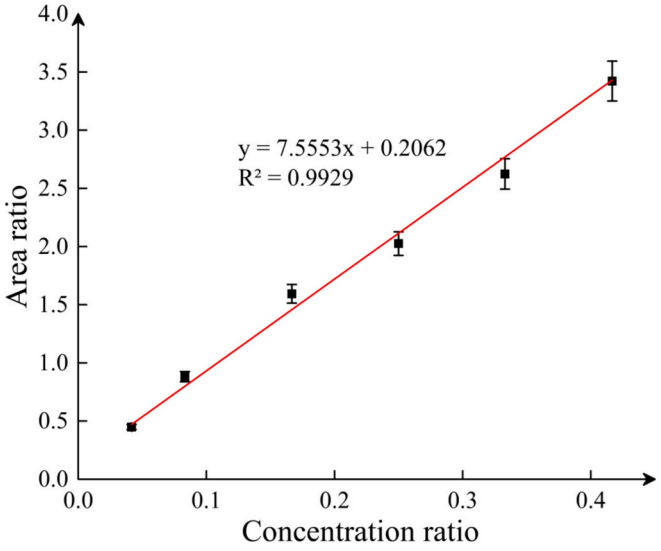

Fig. 6. The linear relationship between the area ratio of clenbuterol to metoprolol and the concentration ratio.

4. Conclusion

A method based on magnetic separation of UCNPs fluorescent probes was developed to detect CLB in pork products. The limits of detection (LOD) and quantification (LOQ) were 0.304 and 1.013 ng mL^{-1}, respectively (LOD = 3 SD/slope and LOQ = 10 SD/slope). This method benefits from the high specificity of the aptamer for specifically recognizing CLB and effective magnetic separation, while the UCNPs provide good fluorescence intensity. Compared with the complex operation of GC–MS, this method is relatively simple, and the prepared materials can be stored for a long time, making their use more convenient.

Funding

This research was supported by Key Research and Development Program of Zhejiang Province (2021C02061) and Chunhui Project Foundation of the Education Department of China (HZKY20220193).

CRediT authorship contribution statement

Xin-Jie Song: Writing – review & editing, Supervision, Project administration, Methodology. **Fei Ye:** Writing – original draft, Methodology, Investigation, Formal analysis. **Yao Zhang:** Validation, Supervision. **Juan Sun:** Validation, Supervision. **Xuping Shentu:** Validation, Supervision, Formal analysis. **Xiaoping Yu:** Validation, Supervision, Investigation. **Wei Li:** Supervision, Methodology, Investigation. **Yuan-Feng Wu:** Validation, Supervision, Funding acquisition, Conceptualization.

Declaration of competing interest

The authors declare that they have no known competing financial interests or personal relationships that could have appeared to influence the work reported in this paper.

Data availability

No data was used for the research described in the article.

Appendix A. Supplementary data

Supplementary data to this article can be found online at https://doi.org/10.1016/j.fochx.2024.101911.

References

Allegrini, F., Olivieri, A., & C.. (2014). IUPAC-consistent approach to the limit of detection in partial least-squares calibration. *Analytical Chemistry, 86*(15), 7858–7866.

Amouroux, B., Roux, C., Micheau, J. C., Gauffre, F., & Coudret, C. (2019). A photochemical determination of luminescence efficiency of upconverting nanoparticles. *Beilstein Journal of Organic Chemistry, 15*, 2671–2677.

Bastos, V., Oskoei, P., Andresen, E., Saleh, M. I., Rühle, B., Resch-Genger, U., & Oliveira, H. (2022). Stability, dissolution, and cytotoxicity of $NaYF_4$-upconversion nanoparticles with different coatings. *Scientific Reports, 12*(1), 3770.

Bayat, P., Nosrati, R., Alibolandi, M., Rafatpanah, H., Abnous, K., Khedri, M., & Ramezani, M. (2018). SELEX methods on the road to protein targeting with nucleic acid aptamers. *Biochimie, 154*, 132–155.

Dou, P., Xiang, Y., Liang, L., & Liu, Z. (2021). Preparation of multi-functional magnetic nanoparticles for harvesting low-molecular-weight glycoproteins. *Se Pu, 39*(10), 1102–1110.

Du, K., Feng, J., Gao, X., & Zhang, H. J. (2022). Nanocomposites based on lanthanide-doped upconversion nanoparticles: Diverse designs and applications. *Light: Science & Applications, 11*(1), 222.

Duan, N., Qi, S., Guo, Y., Xu, W., Wu, S. J., & Wang, Z. P. (2020). Fe_3O_4@Au@Ag nanoparticles as surface-enhanced Raman spectroscopy substrates for sensitive detection of clenbuterol hydrochloride in pork with the use of aptamer binding. *LWT, 134*, 110017.

Guo, Q., Peng, Y., Chao, K., Qin, J., Chen, Y., & Yin, T. (2023). A determination method for clenbuterol residue in pork based on optimal particle size gold colloid using SERS. *Spectrochimica Acta. Part A, Molecular and Biomolecular Spectroscopy, 302*, 123097.

Herpin, L., Bichon, E., Rambaud, L., Monteau, F., & Le Bizec, B. (2018). Comparison between liquid chromatography and supercritical fluid chromatography coupled to mass spectrometry for beta-agonists screening in feeding stuff. *Journal of Chromatography B, 1086*, 130–137.

Himmelstoß, S. F., & Hirsch, T. (2019). A critical comparison of lanthanide based upconversion nanoparticles to fluorescent proteins, semiconductor quantum dots, and carbon dots for use in optical sensing and imaging. *Methods and Applications in Fluorescence, 7*(2), Article 022002.

Jin, X. C., Fang, G. Z., Pan, M. F., Yang, Y. K., BAI, X. Y., & Wang, S. (2018). A molecularly imprinted electrochemiluminescence sensor based on upconversion nanoparticles enhanced by electrodeposited rGO for selective and ultrasensitive detection of clenbuterol. *Biosensors and Bioelectronics, 102*, 357–364.

Jin, Z., Sheng, W., Huang, N., Ren, L. S., SUN, M. Y., Bai, D. M., … Ya, T. T. (2023). Blue-green-red multicolor upconversion nanoparticles based fluorescence immunoassay for simultaneous detection of three mycotoxins in cereals. *Microchemical Journal, 193*, 109181.

Li, Y., Zhang, H., Cui, Z., Liu, S., Xu, J., Jia, C, … Wang, J. (2023). Chemical staining enhanced enzyme-linked immunosorbent assay for sensitive determination of Clenbuterol in food. *Food Chemistry, 400*, 134012.

Liu, H., Li, H., Xia, S., Yu, S. S., Duan, Y. J., Wang, L., … He, H. (2023). Design of a cellulose nanocrystal-based upconversion ratiometric fluorescent nanoprobe for pH monitoring and imaging. *Chemical Engineering Journal, 454*, 140456.

Liu, Y., Lu, Q., Hu, X., Wang, H., Li, H., Zhang, Y., & Yao, S. (2017). A nanosensor based on carbon dots for recovered fluorescence detection Clenbuterol in pork samples. *Journal of Fluorescence, 27*(5), 1847–1853.

Liu, Y., Zhang, C., Liu, H., Li, Y. B., Xu, Z. S., Li, L., & Whittaker, A. (2018). Controllable synthesis of up-conversion nanoparticles UCNPs@MIL-PEG for pH-responsive drug delivery and potential up-conversion luminescence/magnetic resonance dual-mode imaging. *Journal of Alloys and Compounds, 749*, 939–947.

Ma, F., Li, X., Li, Y., Feng, Y., & Ye, B. C. (2022). High current flux electrochemical sensor based on nickel-iron bimetal pyrolytic carbon material of paper waste pulp for clenbuterol detection. *Talanta, 250*, 123756.

Ma, L., Nilghaz, A., Choi, J. R., Liu, X., & Lu, X. (2018). Rapid detection of clenbuterol in milk using microfluidic paper-based ELISA. *Food Chemistry, 246*, 437–441.

Mason, D. M., Friedensohn, S., Weber, C. R., Jordi, C., Wagner, B., Meng, S. M., … Reddy, S. T. (2021). Optimization of therapeutic antibodies by predicting antigen specificity from antibody sequence via deep learning. *Nature Biomedical Engineering, 5*(6), 600–612. https://doi.org/10.1038/s41551-021-00699-9

Midkiff, K. (2004). *The meat you eat: How corporate farming has endangered america's food supply*. St. Martin's Press.

Py, G., Ramonatxo, C., Sirvent, P., Sanchez, A. M. J., Philippe, A. G., Douillard, A., … Candau, R. B. (2015). Chronic clenbuterol treatment compromises force production without directly altering skeletal muscle contractile machinery. *The Journal of Physiology, 593*(8), 2071–2084.

Rafique, R., Kailasa, S. K., & Park, T. J. (2019). Recent advances of upconversion nanoparticles in theranostics and bioimaging applications. *TrAC Trends in Analytical Chemistry, 120*, Article 115646, 2019/11/01/ 2019.

Rubio, L. M. S., Hernández Chávez, J. F., Ruíz López, F. A., Medina, M. R., Delgado, S. E., Méndez, M. R. D., & Ngapo, T. M. (2020). Horse meat sold as beef and consequent clenbuterol residues in the unregulated Mexican marketplace. *Food Control, 110*, 107028.

Sargazi, S., Fatima, I., Hassan, K. M., Mohammadzadeh, V., Arshad, R., Bilal, M., … Behzadmehr, R. (2022). Fluorescent-based nanosensors for selective detection of a wide range of biological macromolecules: A comprehensive review. *International Journal of Biological Macromolecules, 206*, 115–147.

Song, N. E., Lee, J. Y., &Mansur, A. R., Jang, H. W., Lim, M. C., Lee, Y., … Nam, T. G. (2019). Determination of 60 pesticides in hen eggs using the QuEChERS procedure followed by LC-MS/MS and GC-MS/MS. *Food Chemistry, 298*, 125050.

Su, L., Hu, H., Tian, Y., Jia, C., Wang, L., Zhang, H., … Zhang, D. (2021). Highly sensitive colorimetric/surface-enhanced Raman spectroscopy immunoassay relying on a metallic Core-Shell Au/Au Nanostar with Clenbuterol as a target analyte. *Analytical Chemistry, 93*(23), 8362–8369.

Wang, H. L., Yan, H., Shi, M. R, Wang, F. Y., Mei, K., Yu, Q., … Wang, X. D. (2015). An enzyme-assisted and nitrogen-blowing salt-induced solidified floating organic droplet microextraction for determination of clenbuterol and ractopamine in swine feed via capillary electrophoresis. *Animal Feed Science and Technology, 209*, 257–267.

Xiao, Y. P., Lu, H. Y., Lü, S. J., Xie, S. X., Wang, Z. Z., & Chen, H. W. (2016). Rapid analysis of trace salbutamol and Clenbuterol in pork samples by mass spectrometry. *Chinese Journal of Analytical Chemistry, 44*(11), 1633–1638.

Yikilmaz, Y., Kuzukiran, O., Erdogan, E., Sen, F., Kirmizibayrak, O., & Filazi, A. (2020). The determination of β-agonist residues in bovine tissues using liquid chromatography-tandem mass spectrometry. *Biomedical Chromatography, 34*(10), e4926.

Zeng, J. Y., Zhang, T., Liang, G. Y., Mo, J. W., Zhu, J. X., Qin, L. H., … Ni, Z. H. (2024). A "turn off–on" fluorescent sensor for detection of Cr(VI) based on upconversion nanoparticles and nanoporphyrin. *Spectrochimica Acta Part A: Molecular and Biomolecular Spectroscopy, 311*, 124002.

Zhang, J. L., Lu, J. H., Zhang, Y., & Wang, Y. (2023). A LC-MS/MS method for determination of clenbuterol enantiomers in animal tissues and its application to the enantioselective distribution in Bama mini-pigs. *Journal of Chromatography B, 1226*, 123790.

Zhang, W., Wang, P. L, & Su, X. O. (2016). Current advancement in analysis of β-agonists. *TrAC Trends in Analytical Chemistry, 85*, 1–16.

Zhao, X., Lu, Y., Li, B., Kong, M. H., Sun, Y. F., Li, H. X., … Lu, G. Y. (2024). Self-ratiometric fluorescent platform based on upconversion nanoparticles for on-site detection of chlorpyrifos. *Food Chemistry, 439*, 138100.

Zhao, Y. (2019). Application of UCNPs in bio-imaging and treatment. In R. Yang (Ed.), *Principles and applications of up-converting phosphor technology* (pp. 235–244). Singapore: Springer.

Zon, G. (2022). Recent advances in aptamer applications for analytical biochemistry. *Analytical Biochemistry, 644*, Article 113894.

Jing, H., Ouyang, H. Y., Li, W. F., & &Long, Y. M. (2022). Molten salt synthesis of BCNO nanosheets for the electrochemical detection of clenbuterol. *Microchemical Journal, 178*, 107359.

Li, J., Ren, X. L, Diao, Y. Y, Chen, Y., Wang, Q. L., Jin, W. T., … Liu, H. M. (2018). Multiclass analysis of 25 veterinary drugs in milk by ultra-high performance liquid chromatography-tandem mass spectrometry. *Food Chemistry, 257*, 259–264.